

Leptoquarks and Matter Unification: Flavor Anomalies and the Muon $g - 2$

Pavel Fileviez Pérez¹, Clara Murgui², Alexis D. Plascencia¹

¹*Physics Department and Center for Education and Research in Cosmology and Astrophysics (CERCA),
Case Western Reserve University, Cleveland, OH 44106, USA*

²*Walter Burke Institute for Theoretical Physics,
California Institute of Technology, Pasadena, CA 91125**

We discuss the minimal theory for quark-lepton unification at the low scale. In this context, the quarks and leptons are unified in the same representations and neutrino masses are generated through the inverse seesaw mechanism. The properties of the leptoquarks predicted in this theory are discussed in detail and we investigate the predictions for the leptonic and semi-leptonic decays of mesons. We study the possibility to explain the current value of \mathcal{R}_K reported by the LHCb collaboration and the value of the muon anomalous magnetic moment reported by the Muon $g - 2$ experiment at Fermilab.

arXiv:2104.11229v1 [hep-ph] 22 Apr 2021

* pxf112@case.edu, cmurgui@caltech.edu, alexis.plascencia@case.edu

1. INTRODUCTION

The idea of quark-lepton unification by J. Pati and A. Salam [1] provides a simple and elegant way to think about unification of matter and interactions in nature. The minimal theory of Pati-Salam is very predictive because it predicts, at the scale where matter unifies, that the masses of the charged leptons and down-quarks are equal, and the masses for the up-quarks are equal to the Dirac masses for neutrinos. Moreover, the $SU(4)_C$ gauge symmetry must be broken around the canonical seesaw scale, 10^{14} GeV, in order to achieve small neutrino masses, via the seesaw mechanism [2–5], in agreement with experiments.

The simplest quark-lepton unification theory that can be realized at the TeV scale was proposed in Ref. [6]. This theory is based on the $SU(4)_C \otimes SU(2)_L \otimes U(1)_R$ gauge group and in order to have a consistent theory for fermion masses at the low scale, neutrino masses are generated through the inverse seesaw mechanism [7, 8]. This theory for quark-lepton unification predicts, among the new fields required for its consistency, the existence of mediators that interact simultaneously with both leptons and quarks. Particularly, this theory predicts a vector leptoquark, $X_\mu \sim (\mathbf{3}, \mathbf{1}, -2/3)_{\text{SM}}$, and two scalar leptoquarks, $\Phi_3 \sim (\bar{\mathbf{3}}, \mathbf{2}, -1/6)_{\text{SM}}$ and $\Phi_4 \sim (\mathbf{3}, \mathbf{2}, 7/6)_{\text{SM}}$, which mediate interesting and exotic processes that could otherwise not be seen in the context of the Standard Model¹. For a review about the phenomenology of leptoquarks see Ref. [9].

Recently, the LHCb collaboration has reported results for the ratio \mathcal{R}_K defined as

$$\mathcal{R}_K = \frac{\text{Br}(B^+ \rightarrow K^+ \mu^+ \mu^-)}{\text{Br}(B^+ \rightarrow K^+ e^+ e^-)},$$

which is predicted to be 1 in the SM. The measurement reported by LHCb [10] using data from Run 2 is

$$\mathcal{R}_K^{\text{exp}}(1.1 < q^2 < 6.0 \text{ GeV}^2) = 0.846_{-0.039}^{+0.042+0.013}_{-0.012}, \quad (1)$$

which is in tension with the SM prediction at 3.1σ . This observable, together with \mathcal{R}_{K^*} and the leptonic decays $\text{Br}(B_s \rightarrow \ell^+ \ell^-)$ are usually classified as *clean observables*; in the former the hadronic effects cancel almost exactly while the long distance effects cancel in the absence of new physics in both observables. These experimental results have motivated many studies in the particle physics community, see e.g. [11–28].

There are also new results reported by the Fermilab Muon $g-2$ experiment on the anomalous magnetic moment of the muon a_μ from their Run 1 [29]. The combined result with the one from the E821 experiment at BNL [30] deviates from the SM prediction by 4.2σ ²

$$\Delta a_\mu = a_\mu^{\text{exp}} - a_\mu^{\text{SM}} = (251 \pm 59) \times 10^{-11}. \quad (2)$$

There have been different proposals of theories beyond the SM to explain this anomaly, see e.g. Refs. [32–43]. These results for \mathcal{R}_K and $(g-2)_\mu$, which are naturally expected if new physics is around the multi-TeV scale, could help us find a new direction for physics beyond the Standard Model.

In this article, we investigate the possibility to explain the experimental value of \mathcal{R}_K in two main scenarios. In the first scenario the scalar leptoquark, $\Phi_3 \sim (\bar{\mathbf{3}}, \mathbf{2}, -1/6)_{\text{SM}}$, gives the main contribution to the relevant meson decays, while in the second scenario the scalar leptoquark,

¹We label with the subscript SM the quantum numbers of the corresponding field under the Standard Model gauge group $SU(3)_C \otimes SU(2)_L \otimes U(1)_Y$. Those where this label is not explicitly written refer to the \mathcal{G}_{QL} gauge group.

²There are results from lattice QCD that are compatible with the experimental value [31].

$\Phi_4 \sim (\mathbf{3}, \mathbf{2}, 7/6)_{\text{SM}}$, plays the main role to explain the value of \mathcal{R}_K . We demonstrate that in the most general case where there is mixing between the scalar leptoquarks there is a contribution to $(g-2)_\mu$ that has no chiral suppression and can explain the reported value by the Muon $g-2$ collaboration. Our main conclusion is that in the context of a simple theory for quark-lepton unification proposed in Ref. [6] one can explain simultaneously the recent experimental results for \mathcal{R}_K and $(g-2)_\mu$. Therefore, one could expect that the leptoquarks have masses around the TeV scale and we can hope to test this theory in the near future.

This article is organized as follows: in Section 2 we discuss the minimal theory for quark-lepton unification at the low scale, in Section 3 we investigate the predictions for meson decays and discuss the different leptoquark candidates to explain the experimental value of \mathcal{R}_K . In Section 4 we discuss the possibility to explain the recent experimental results for the $g-2$ of the muon, and discuss the correlation between the predictions for \mathcal{R}_K and $(g-2)_\mu$. Finally, in Section 5 we summarize our main findings.

2. MINIMAL THEORY FOR QUARK-LEPTON UNIFICATION

The minimal theory for quark-lepton unification that can describe physics at the TeV scale was proposed in Ref. [6]. This theory is based on the gauge symmetry,

$$\mathcal{G}_{QL} = \text{SU}(4)_C \otimes \text{SU}(2)_L \otimes \text{U}(1)_R,$$

and the SM matter fields are unified as

$$F_{QL} = \begin{pmatrix} u & \nu \\ d & e \end{pmatrix} \sim (\mathbf{4}, \mathbf{2}, 0), \quad F_u = \begin{pmatrix} u^c & \nu^c \end{pmatrix} \sim (\bar{\mathbf{4}}, \mathbf{1}, -1/2), \quad (3)$$

$$\text{and} \quad F_d = \begin{pmatrix} d^c & e^c \end{pmatrix} \sim (\bar{\mathbf{4}}, \mathbf{1}, 1/2). \quad (4)$$

Here all the SM fields and ν^c are in the left-handed representation, and the unification for quarks and leptons is for each SM family. This theory can be seen as a low energy limit of the Pati-Salam model based on $\text{SU}(4)_C \otimes \text{SU}(2)_L \otimes \text{SU}(2)_R$, when the $\text{SU}(2)_R$ symmetry is broken to $\text{U}(1)_R$. One can also obtain the gauge symmetry \mathcal{G}_{QL} from a theory based on $\text{SU}(6)$.

In this theory the gauge fields live in

$$A_\mu = \begin{pmatrix} G_\mu & X_\mu/\sqrt{2} \\ X_\mu^*/\sqrt{2} & 0 \end{pmatrix} + T_4 B'_\mu \sim (\mathbf{15}, \mathbf{1}, 0), \quad (5)$$

where $G_\mu \sim (\mathbf{8}, \mathbf{1}, 0)_{\text{SM}}$ are the gluons, $X_\mu \sim (\mathbf{3}, \mathbf{1}, 2/3)_{\text{SM}}$ are vector leptoquarks, and $B'_\mu \sim (\mathbf{1}, \mathbf{1}, 0)_{\text{SM}}$. The Higgs sector is composed of three Higgses, Φ and χ and the SM Higgs H ,

$$H^T = (H^+ \ H^0) \sim (\mathbf{1}, \mathbf{2}, 1/2), \quad \chi = (\chi_u \ \chi_R^0) \sim (\mathbf{4}, \mathbf{1}, 1/2), \quad \text{and} \\ \Phi = \begin{pmatrix} \Phi_8 & \Phi_3 \\ \Phi_4 & 0 \end{pmatrix} + T_4 H_2 \sim (\mathbf{15}, \mathbf{2}, 1/2). \quad (6)$$

Here $H_2 \sim (\mathbf{1}, \mathbf{2}, 1/2)_{\text{SM}}$ is a second Higgs doublet, $\Phi_8 \sim (\mathbf{8}, \mathbf{2}, 1/2)_{\text{SM}}$, and the scalar leptoquarks $\Phi_3 \sim (\bar{\mathbf{3}}, \mathbf{2}, -1/6)_{\text{SM}}$ and $\Phi_4 \sim (\mathbf{3}, \mathbf{2}, 7/6)_{\text{SM}}$. The T_4 generator of $\text{SU}(4)_C$ in the above equation is normalized as $T_4 = \frac{1}{2\sqrt{6}} \text{diag}(1, 1, 1, -3)$. The \mathcal{G}_{QL} gauge group is spontaneously broken to the

SM gauge group by the vacuum expectation value (VEV) of the scalar field $\langle \chi_R^0 \rangle = v_\chi/\sqrt{2}$, which gives mass to the vector leptoquark X_μ , defining the scale of matter unification.

The Yukawa interactions in this theory are given by

$$-\mathcal{L}_{QL}^Y = Y_1 F_{QL} F_u H + Y_2 F_{QL} F_u \Phi + Y_3 H^\dagger F_{QL} F_d + Y_4 \Phi^\dagger F_{QL} F_d + \text{h.c.}, \quad (7)$$

and the mass matrices for the SM fermions read as

$$M_u = Y_1 \frac{v_1}{\sqrt{2}} + \frac{1}{2\sqrt{6}} Y_2 \frac{v_2}{\sqrt{2}}, \quad M_\nu^D = Y_1 \frac{v_1}{\sqrt{2}} - \frac{3}{2\sqrt{6}} Y_2 \frac{v_2}{\sqrt{2}}, \quad (8)$$

$$M_d = Y_3 \frac{v_1}{\sqrt{2}} + \frac{1}{2\sqrt{6}} Y_4 \frac{v_2}{\sqrt{2}}, \quad M_e = Y_3 \frac{v_1}{\sqrt{2}} - \frac{3}{2\sqrt{6}} Y_4 \frac{v_2}{\sqrt{2}}. \quad (9)$$

Here the VEVs of the Higgs doublets are defined as $\langle H^0 \rangle = v_1/\sqrt{2}$, and $\langle H_2^0 \rangle = v_2/\sqrt{2}$. Notice that without the scalar field Φ one cannot generate a consistent relation for charged fermion masses. Now, in order to generate small neutrino masses at the low scale one needs to go beyond the canonical seesaw mechanism. We can generate small Majorana masses for the light neutrinos if we add three new singlet left-handed fermionic fields $S \sim (\mathbf{1}, \mathbf{1}, 0)$ and use the following interaction terms [6], which emerge in the Lagrangian once the fermion singlets are included,

$$-\mathcal{L}_{QL}^\nu = Y_5 F_u \chi S + \frac{1}{2} \mu S S + \text{h.c.} \quad (10)$$

In this case the mass matrix for neutrinos in the basis (ν, ν^c, S) reads as

$$(\nu \ \nu^c \ S) \begin{pmatrix} 0 & M_\nu^D & 0 \\ (M_\nu^D)^T & 0 & M_\chi^D \\ 0 & (M_\chi^D)^T & \mu \end{pmatrix} \begin{pmatrix} \nu \\ \nu^c \\ S \end{pmatrix}. \quad (11)$$

Here M_ν^D is given by Eq. (8) and $M_\chi^D = Y_5 v_\chi/\sqrt{2}$. The light neutrino mass is given by

$$m_\nu \approx \mu (M_\nu^D)^2 / (M_\chi^D)^2, \quad (12)$$

if $M_\chi^D \gg M_\nu^D \gg \mu$ holds. Such hierarchy is motivated by the different scales of the theory: $M_\chi^D \propto v_\chi$, which determines the scale of matter unification, $M_\nu^D \propto v_{1,2}$, which define the electroweak scale, and μ is instead protected by a fermion symmetry, so that it is technically natural to assume it small. Notice that neutrinos would be massless in the limit $\mu \rightarrow 0$, which is the usual relation in the inverse seesaw mechanism.

The vector leptoquarks, $X_\mu \sim (\mathbf{3}, \mathbf{1}, 2/3)_{\text{SM}}$, have the following interactions

$$\mathcal{L} \supset \frac{g_4}{\sqrt{2}} X_\mu (\bar{Q}_L \gamma^\mu \ell_L + \bar{u}_R \gamma^\mu \nu_R + \bar{d}_R \gamma^\mu e_R) + \text{h.c.}, \quad (13)$$

where the gauge coupling g_4 is equal to the strong coupling constant evaluated at the $\text{SU}(4)_C$ scale, and $(\nu_R)^C = (\nu^C)_L$. See Appendix A for details of the interactions in the physical basis.

The Yukawa interactions in Eq. (7), other than generating the mass of the fermions, contain new Yukawa interactions with respect to the Standard Model. Particularly, the predicted scalar leptoquarks, $\Phi_3 \sim (\bar{\mathbf{3}}, \mathbf{2}, -1/6)_{\text{SM}}$ and $\Phi_4 \sim (\mathbf{3}, \mathbf{2}, 7/6)_{\text{SM}}$, have the following interactions with

quarks and leptons,

$$-\mathcal{L}_{QL}^Y \supset Y_2 Q_L \Phi_3 (\nu^c)_L + Y_2 \ell_L \Phi_4 (u^c)_L + Y_4 \ell_L \Phi_3^\dagger (d^c)_L + Y_4 Q_L \Phi_4^\dagger (e^c)_L + \text{h.c.} \quad (14)$$

We note that neutrino masses can be small even when $Y_2 \rightarrow 0$, due to the inverse seesaw mechanism, but the entries in Y_4 cannot be arbitrarily small because one needs a realistic relation between down quarks and charged lepton masses,

$$Y_4 = \frac{\sqrt{3}}{v_2} (M_d - M_e). \quad (15)$$

The scalar leptoquarks Φ_3 and Φ_4 can be written in $\text{SU}(2)_L$ components as,

$$\Phi_3 = \begin{pmatrix} \phi_3^{1/3} \\ \phi_3^{-2/3} \end{pmatrix}, \text{ and } \Phi_4 = \begin{pmatrix} \phi_4^{5/3} \\ \phi_4^{2/3} \end{pmatrix}, \quad (16)$$

where the numbers in parenthesis denote the electric charge. In Appendix A we present the interactions of the leptoquarks in the physical basis, where the fermions are mass eigenstates. For some phenomenological studies of this theory see for example Refs. [21, 44].

3. MESON DECAYS: \mathcal{R}_K AND \mathcal{R}_{K^*}

The theory predicts the existence of a vector leptoquark, X_μ , and two scalar leptoquarks, Φ_3 and Φ_4 , among other fields. The interactions of the X_μ leptoquark are determined by the unitary mixing matrix V_{DE} , see Appendix A for details. Unfortunately, one cannot explain easily the values of \mathcal{R}_K and satisfy the bounds from the experimental constraints on $K_L \rightarrow e^\pm \mu^\mp$ when the mixing matrix is unitary. See the studies in Refs. [21, 26] for details. Consequently, we focus our study on the scalar leptoquarks that the theory predicts.

The interactions of the scalar leptoquarks with the Standard Model fermions are needed to render the fermion masses realistic, and therefore cannot be assumed small. In particular, in Eqs. (8) and (9) one can see that Y_2 can be neglected, but Y_4 must be non-zero in order to have a consistent relation between the charged leptons and down quarks masses. For simplicity, in this work we will study scenarios where we take the limit $Y_2 \rightarrow 0$, and hence, the interactions of the scalar leptoquarks with the Standard Model fermions are given by

$$-\mathcal{L}_Y = Y_4^{ab} \left(\bar{d}_R^b (\phi_3^{1/3})^* \nu_L^a + \bar{d}_R^b (\phi_3^{-2/3})^* e_L^a + \bar{e}_R^b (\phi_4^{5/3})^* u_L^a + \bar{e}_R^b (\phi_4^{2/3})^* d_L^a \right) + \text{h.c.}, \quad (17)$$

which in the basis where the fermions are mass eigenstates read,

$$\begin{aligned} -\mathcal{L}_Y = & \bar{d}_R^b V_4^{ab} (\phi_3^{1/3})^* \nu_L^a + \bar{d}_R^b (K_3^* V_{\text{PMNS}}^* V_4)^{ab} (\phi_3^{-2/3})^* e_L^a \\ & + \bar{e}_R^b V_6^{ab} (\phi_4^{5/3})^* u_L^a + \bar{e}_R^b (K_2 V_{\text{CKM}}^T K_1 V_6)^{ab} (\phi_4^{2/3})^* d_L^a + \text{h.c.} \end{aligned} \quad (18)$$

To determine the parameters quantifying the leptoquark interaction with fermions, i.e. the corresponding coupling and the leptoquark mass, the predictions of the theory should be contrasted with experimental measurements. Strikingly, both scalar leptoquarks contribute to $b \rightarrow s$ transitions through their coupling between the charged leptons and down quarks, via the $\phi_3^{-2/3}$ and $\phi_4^{2/3}$ fields. Therefore, in the light of the recent deviations reported by the LHCb on such

transitions, we should ask the theory to accommodate the experimental results, being the largest deviation 3.1σ in the clean observable \mathcal{R}_K . In the following phenomenological analysis we are only considering the clean observables; namely, the ratios $\mathcal{R}_{K^{(*)}}$ and the branching fraction of the leptonic decays $\text{Br}(B_s \rightarrow \ell^+ \ell^-)$. Furthermore, by accommodating the experimental results on those observables, the theory predicts other flavour processes that could be tested at current or upcoming experiments.

A. Scalar Leptoquark $\phi_3^{-2/3}$

The scalar leptoquark $\phi_3^{-2/3}$ contributes to the following dimension 6 effective interactions

$$\mathcal{L}_{\text{eff}}^{\phi_3^{-2/3}} \supset \frac{4G_F}{\sqrt{2}} V_{tb} V_{ts}^* \frac{\alpha}{4\pi} [C'_{9\ell\ell} (\bar{s}\gamma_\mu P_R b)(\bar{\ell}\gamma^\mu \ell) + C'_{10\ell\ell} (\bar{s}\gamma_\mu P_R b)(\bar{\ell}\gamma^\mu \gamma^5 \ell)] + \text{h.c.}, \quad (19)$$

whose Wilson coefficients are determined after integrating $\phi_3^{-2/3}$ out and are given by

$$\begin{aligned} C'_{10\ell\ell} = -C'_{9\ell\ell} &= \left(\frac{\sqrt{2}\pi}{G_F V_{tb} V_{ts}^* \alpha} \right) \frac{(K_3^* V_{\text{PMNS}}^* V_4)^{\ell 3} (K_3 V_{\text{PMNS}} V_4^*)^{\ell 2}}{4M_{\phi_3^{-2/3}}^2} \\ &\simeq (36 \text{ TeV})^2 \frac{(K_3^* V_{\text{PMNS}}^* V_4)^{\ell 3} (K_3 V_{\text{PMNS}} V_4^*)^{\ell 2}}{4M_{\phi_3^{-2/3}}^2}. \end{aligned} \quad (20)$$

The fact that the theory predicts $C'_{10\ell\ell} = -C'_{9\ell\ell}$ allows us to write the leptonic branching ratio $B_s \rightarrow \ell^+ \ell^-$ as a function of a single Wilson coefficient $C'_{10\ell\ell}$,

$$\text{Br}(B_s \rightarrow \ell^+ \ell^-) = \text{Br}(B_s \rightarrow \ell\ell)_{\text{SM}} \times (1 + 0.4875 \text{Re}[C'_{10\ell\ell}] + 0.05940 |C'_{10\ell\ell}|^2), \quad (21)$$

where for the Standard Model prediction we take $\text{Br}(B_s \rightarrow \mu^+ \mu^-)_{\text{SM}} = 3.66 \times 10^{-9}$ [45] and $\text{Br}(B_s \rightarrow e^+ e^-)_{\text{SM}} = 8.35 \times 10^{-14}$ [46, 47]. The same applies to the rest of the clean observables we are considering³,

$$\mathcal{R}_K = \mathcal{R}_K^{\text{SM}} \frac{1 - 0.5040 \text{Re}[C'_{10\mu\mu}] + 0.06359 |C'_{10\mu\mu}|^2}{1 - 0.5040 \text{Re}[C'_{10ee}] + 0.06359 |C'_{10ee}|^2} \quad \text{for } q^2 \in [1.1, 6] \text{ GeV}^2, \quad (22)$$

$$\mathcal{R}_{K^*} = \mathcal{R}_{K^*}^{\text{SM}} \frac{1 + 0.4335 \text{Re}[C'_{10\mu\mu}] + 0.07473 |C'_{10\mu\mu}|^2}{1 + 0.4325 \text{Re}[C'_{10ee}] + 0.07472 |C'_{10ee}|^2} \quad \text{for } q^2 \in [1.1, 6] \text{ GeV}^2, \quad (23)$$

$$\mathcal{R}_{K^*} = \mathcal{R}_{K^*}^{\text{SM}} \frac{1 + 0.2363 \text{Re}[C'_{10\mu\mu}] + 0.03266 |C'_{10\mu\mu}|^2}{1 + 0.2252 \text{Re}[C'_{10ee}] + 0.03127 |C'_{10ee}|^2} \quad \text{for } q^2 \in [0.045, 1.1] \text{ GeV}^2. \quad (24)$$

In Fig. 1 we show the parameter space in the $\text{Br}(B_s \rightarrow \mu^+ \mu^-)$ vs $\text{Br}(B_s \rightarrow e^+ e^-)$ plane that satisfies the experimental value of \mathcal{R}_K at the 1σ level [10], see Eq. (1). We note that, due to the quadratic dependence of the observables on $C'_{10\ell\ell}$, for a given $\text{Br}(B_s \rightarrow \mu^+ \mu^-)$ and $\text{Br}(B_s \rightarrow e^+ e^-)$ there exist four possible values of \mathcal{R}_K allowed. In this figure present the solution that is also consistent with the measured window for \mathcal{R}_K . We also take into account the existing experimental

³For the calculation of the ratios \mathcal{R}_K and \mathcal{R}_{K^*} we adopt the form factors from Ref. [48] and Ref. [49], respectively.

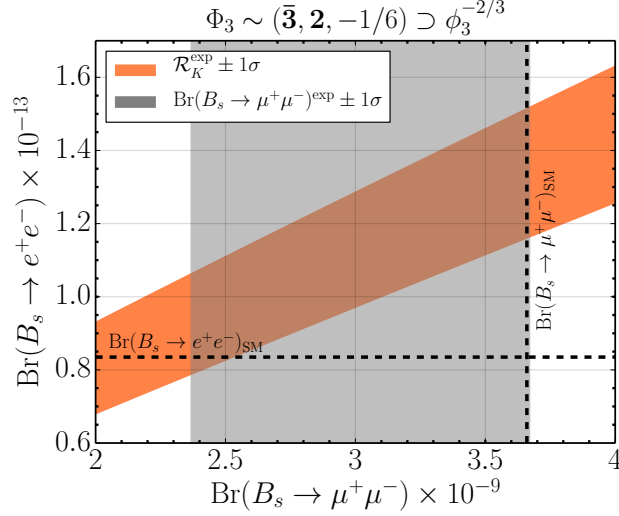


FIG. 1: The orange band gives the correlation between $\text{Br}(B_s \rightarrow e^+e^-)$ and $\text{Br}(B_s \rightarrow \mu^+\mu^-)$ that explains the \mathcal{R}_K experimental measurement within 1σ . The gray band corresponds to the measurement of $\text{Br}(B_s \rightarrow \mu^+\mu^-)$ within 1σ .

bounds on the leptonic decay to muons [50] and to electrons [51], which are given by

$$\text{Br}(B_s \rightarrow \mu^+\mu^-)^{\text{exp}} = 3.0 \pm 0.6_{-0.2}^{+0.3} \times 10^{-9}, \quad (25)$$

$$\text{Br}(B_s \rightarrow e^+e^-)^{\text{exp}} < 2.8 \times 10^{-7}. \quad (26)$$

The region shaded in gray in Fig. 1 shows explicitly the parameter space satisfying $\text{Br}(B_s \rightarrow \mu^+\mu^-)^{\text{exp}}$ [50] at the 1σ level. As the figure shows, we find that there is a region of the parameter space that satisfies $\mathcal{R}_K^{\text{exp}}$ and $\text{Br}(B_s \rightarrow \mu^+\mu^-)^{\text{exp}}$ at 1σ which corresponds to the overlapping region between the regions shaded in gray and in orange in the plot.

In Fig. 2 we plot the correlation between the semileptonic ratios for the different q^2 ranges tested at experiment for the values of $\text{Br}(B_s \rightarrow \mu^+\mu^-)$ and $\text{Br}(B_s \rightarrow e^+e^-)$ consistent with the

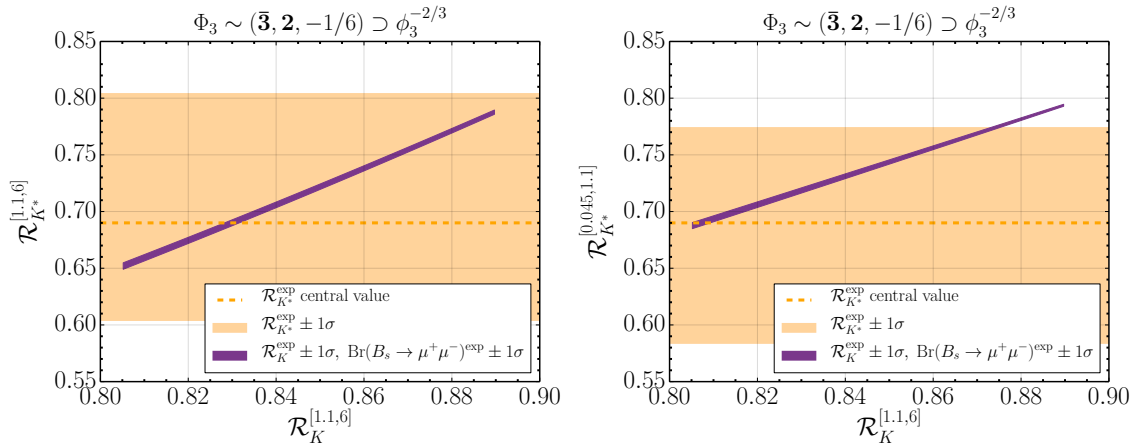


FIG. 2: The purple band gives the prediction for \mathcal{R}_{K^*} in the window $0.045 < q^2 < 1.1 \text{ GeV}^2$ (left panel) and $1.1 < q^2 < 6 \text{ GeV}^2$ (right panel) for the points satisfying $\mathcal{R}_K^{\text{exp}}$ and $\text{Br}(B_s \rightarrow \mu^+\mu^-)^{\text{exp}}$ within 1σ . The region shaded in orange corresponds to the measurement of \mathcal{R}_{K^*} at 1σ .

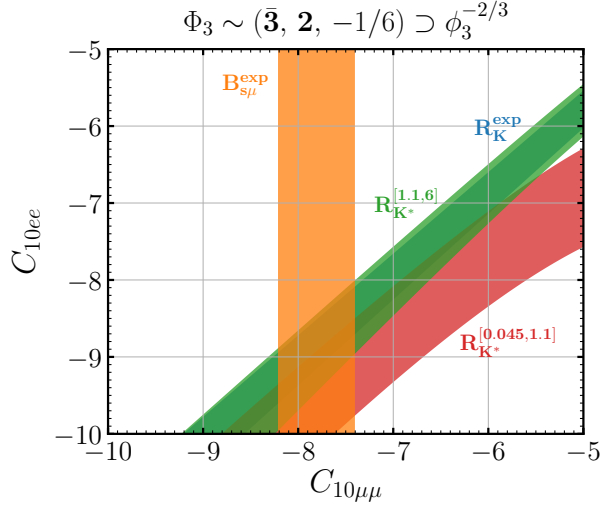


FIG. 3: Parameter space of the Wilson coefficients C_{10ee} and $C_{10\mu\mu}$ required to explain the flavor anomalies. The orange band is in agreement with the measurement of $\text{Br}(B_s \rightarrow \mu^+\mu^-)$ within 1σ . The green (blue and red) band correspond to the measurement of \mathcal{R}_K (\mathcal{R}_{K^*}) within 1σ .

experimental values of $\mathcal{R}_K^{\text{exp}}$ and $\text{Br}(B_s \rightarrow \mu^+\mu^-)^{\text{exp}}$ at the 1σ level. We note that the theory predicts a window for \mathcal{R}_{K^*} that is consistent with the experimental values of this observable [52],

$$\mathcal{R}_{K^*}^{\text{exp}} = \begin{cases} 0.66_{-0.07}^{+0.11} \text{ (stat)} \pm 0.03 \text{ (syst)} & \text{for } 0.045 < q^2 < 1.1 \text{ GeV}^2, \\ 0.69_{-0.07}^{+0.11} \text{ (stat)} \pm 0.05 \text{ (syst)} & \text{for } 1.1 < q^2 < 6.0 \text{ GeV}^2. \end{cases} \quad (27)$$

which deviate from the Standard Model prediction by 2.2σ and 2.4σ , respectively. As Fig. 2 shows, for $1.1 < q^2 < 6 \text{ GeV}^2$ the full predicted window is in agreement with the experimental measurement, while for $0.045 < q^2 < 1.1 \text{ GeV}^2$, the theory prefers lower values of \mathcal{R}_K inside the 1σ range of its experimental value.

Fig. 3 shows the parameter space in the plane of the relevant Wilson coefficients $C_{10\mu\mu}$ and C_{10ee} that satisfies the experimental value of the clean observables at the 1σ level: $\text{Br}(B_s \rightarrow \mu^+\mu^-)^{\text{exp}}$ in orange, $\mathcal{R}_K^{\text{exp}}$ in blue, $\mathcal{R}_{K^*}^{\text{exp}}[1.1, 6]$ in green, and $\mathcal{R}_{K^*}^{\text{exp}}[0.045, 1.1]$ in red, where between brackets we specify the window of the integrated q^2 .

As we have shown in this subsection, the simplest theory where one can understand unification of matter at the TeV scale naturally accommodates the so-called flavour anomalies in $b \rightarrow s$ transitions observed at experiment. As one can read from the Wilson coefficients in Eq. 20, such transitions particularly imply the presence of four entries in the Yukawa matrix between the charged leptons and the down quarks, which in the physical basis reads as $\tilde{Y}_4 \equiv K_3^* V_{\text{PMNS}}^* V_4$, as can be read from Eq. (18). However, the rest of the couplings in this matrix may lead to other flavour transitions, such as $K_L \rightarrow \mu^\pm e^\mp$ and τ decays to light mesons and a charged lepton, which suffer from strong experimental constraints. Requiring consistency with the experiment allows us to infer the texture of the Yukawa matrix \tilde{Y}_4 . By adopting the following hierarchy in their entries,

$$\tilde{Y}_4 = \begin{pmatrix} \cdot & \boxed{} & \boxed{} \\ \cdot & \boxed{} & \boxed{} \\ \cdot & \cdot & \cdot \end{pmatrix}, \quad (28)$$

where the squares denote large entries while the dots denote small entries. Then, the theory can accommodate the experimental values of the clean observables involving $b \rightarrow s$ transitions while being consistent with all existing flavour constraints. Notice that lepton flavour violation processes such as the radiative decays $\mu \rightarrow e\gamma$, $\mu - e$ conversion or the muon magnetic moment $(g - 2)_\mu$ do not offer relevant constraints to the four entries involved in $b \rightarrow s$ transitions since they suffer from the muon mass suppression needed to flip the chirality in the muons. We refer the reader to Sec. 4 for more details. The leptoquark $\phi_3^{-2/3}$ can also induce the decays $B \rightarrow K\mu^\pm e^\mp$ and $B_s \rightarrow \mu^\pm e^\mp$; however, these decays depend on a different combination of couplings than the ones that enter in $\mathcal{R}_{K^{(*)}}$, and hence, there exists enough freedom in the Wilson coefficients for this decay to satisfy the experimental constraint.

On the other hand, we note that $\phi_3^{1/3}$, which also belongs to the $SU(2)_L$ doublet in Eq. (18), shares the entries of \tilde{Y}_4 up to the effect of the V_{PMNS} and some complex diagonal phases. Knowing the texture of \tilde{Y}_4 from the interactions involving $\phi_3^{-2/3}$, the theory predicts a modification of processes such as $B \rightarrow K^{(*)} + \text{missing energy}$, and $B_s \rightarrow \text{missing energy}$ which will depend on the mass of the right-handed neutrinos. The latter are generically heavy in this theory.

B. Scalar Leptoquark $\phi_4^{2/3}$

The scalar leptoquark $\phi_4^{2/3}$ contributes to the following dimension 6 effective interactions,

$$\mathcal{L}_{\text{eff}}^{\phi_4^{2/3}} = \frac{4G_F}{\sqrt{2}} \frac{\alpha}{4\pi} [C_{9\ell\ell}(\bar{s}\gamma_\mu P_L b)(\bar{\ell}\gamma^\mu \ell) + C_{10\ell\ell}(\bar{s}\gamma_\mu P_L b)(\bar{\ell}\gamma^\mu \gamma_5 \ell)] + \text{h.c.}, \quad (29)$$

where the Wilson coefficients are given by

$$C_{10\ell\ell} = C_{9\ell\ell} = - \left(\frac{\pi\sqrt{2}}{G_F V_{tb} V_{ts}^* \alpha} \right) \frac{(K_2 V_{\text{CKM}}^T K_1 V_6)^{3\ell} (K_2^* V_{\text{CKM}}^\dagger K_1^* V_6^*)^{2\ell}}{4M_{\phi_4^{2/3}}^2}. \quad (30)$$

In this case the leptonic branching ratio is also given as a function of a single Wilson coefficient, $C_{10\ell\ell}$,

$$\text{Br}(B_s \rightarrow \ell^+ \ell^-) = \text{Br}(B_s \rightarrow \ell^+ \ell^-)_{\text{SM}} \times (1 - 0.487448 \text{Re}[C_{10\ell\ell}] + 0.0594014|C_{10\ell\ell}|^2), \quad (31)$$

as well as the other clean observables we consider,

$$\mathcal{R}_K = \mathcal{R}_K^{\text{SM}} \frac{1 - 0.01812 \text{Re}[C_{10\mu\mu}] + 0.06359|C_{10\mu\mu}|^2}{1 - 0.01781 \text{Re}[C_{10ee}] + 0.06359|C_{10ee}|^2} \quad \text{for } q^2 \in [1.1, 6] \text{ GeV}^2, \quad (32)$$

$$\mathcal{R}_{K^*} = \mathcal{R}_{K^*}^{\text{SM}} \frac{1 - 0.08301 \text{Re}[C_{10\mu\mu}] + 0.07473|C_{10\mu\mu}|^2}{1 - 0.08428 \text{Re}[C_{10ee}] + 0.07472|C_{10ee}|^2} \quad \text{for } q^2 \in [1.1, 6] \text{ GeV}^2, \quad (33)$$

$$\mathcal{R}_{K^*} = \mathcal{R}_{K^*}^{\text{SM}} \frac{1 - 0.04783 \text{Re}[C_{10\mu\mu}] + 0.03266|C_{10\mu\mu}|^2}{1 - 0.04600 \text{Re}[C_{10ee}] + 0.03127|C_{10ee}|^2} \quad \text{for } q^2 \in [0.045, 1.1] \text{ GeV}^2. \quad (34)$$

In the left panel of Fig. 4 we show our results in the the plane of the Wilson coefficients C_{10ee} vs $C_{10\mu\mu}$. The two orange bands reproduce the measured value for $\text{Br}(B_s \rightarrow \mu^+ \mu^-)$ within 1σ . For the solution with small Wilson coefficients there is a small overlap with the measured values of \mathcal{R}_K and \mathcal{R}_{K^*} . On the other hand, for the solution with larger values for the Wilson coefficients

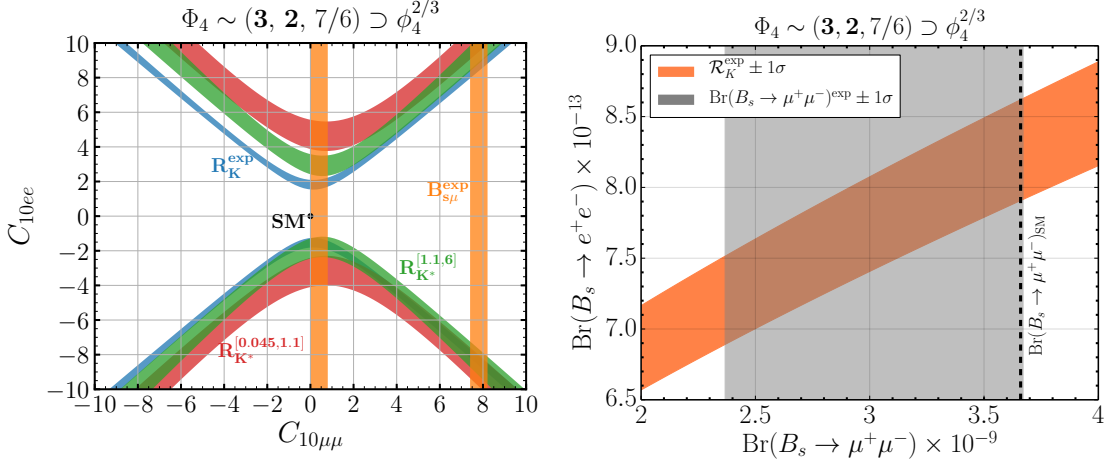


FIG. 4: *Left panel:* . Parameter space of the Wilson coefficients C_{10ee} and $C_{10\mu\mu}$ required to explain the flavor anomalies. The orange band is in agreement with the measurement of $\text{Br}(B_s \rightarrow \mu^+\mu^-)$ within 1σ . The blue, green and red bands correspond to the measurements of \mathcal{R}_K , $\mathcal{R}_{K^*}^{[1.1,6]}$ and $\mathcal{R}_{K^*}^{[0.045,1.1]}$ within 1σ , respectively. *Right panel:* The orange band gives the correlation between $\text{Br}(B_s \rightarrow e^+e^-)$ and $\text{Br}(B_s \rightarrow \mu^+\mu^-)$ that explains the \mathcal{R}_K experimental measurement within 1σ . The gray band corresponds to the measurement of $\text{Br}(B_s \rightarrow \mu^+\mu^-)$ within 1σ .

there is a larger overlap that is also able to explain both \mathcal{R}_K and \mathcal{R}_{K^*} .

In the right panel of Fig. 4 we show the parameter space in the $\text{Br}(B_s \rightarrow \mu^+\mu^-)$ vs $\text{Br}(B_s \rightarrow e^+e^-)$ plane that fulfils $\mathcal{R}_K^{\text{exp}}$ (orange band) and $\text{Br}(B_s \rightarrow \mu^+\mu^-)^{\text{exp}}$ (gray band) at 1σ . For this plot we focus on the solution with large positive $C_{10\mu\mu}$ and negative C_{10ee} values for the Wilson coefficients. In Fig. 5 we show the correlation predicted for the ratios \mathcal{R}_{K^*} and \mathcal{R}_K . In the left panel we give the predictions for \mathcal{R}_{K^*} in the window $1.1 < q^2 < 6 \text{ GeV}^2$, where the purple band is in agreement with \mathcal{R}_K and $\text{Br}(B_s \rightarrow \mu^+\mu^-)^{\text{exp}}$ within 1σ . In the right panel we show the predictions for \mathcal{R}_{K^*} in the window $0.045 < q^2 < 1.1 \text{ GeV}^2$.

Similarly to the previous scenario, the following texture in the Yukawa matrix $\tilde{Y}'_4 = K_2 V_{\text{CKM}}^T K_1 V_6$ mediating the interactions between charged leptons and down quarks must be adopted,

$$\tilde{Y}'_4 = \begin{pmatrix} \ddot{\square} & \ddot{\square} & \vdots \\ \ddot{\square} & \ddot{\square} & \vdots \end{pmatrix}, \quad (35)$$

in order to avoid the strong experimental constraints in other flavour transitions such as $K_L \rightarrow e^\pm \mu^\mp$ or τ decays to light mesons and charged leptons. As in the case of Φ_3 , since we are neglecting interactions mediated by Y_2 , there is no relevant contribution from this scalar leptoquark to the $\mu \rightarrow e\gamma$, $\mu - e$ conversion or $(g-2)_\mu$. We note that in the case with both Y_2 and Y_4 large, the scalar leptoquark Φ_4 could give a relevant contribution to those kind of processes since then it will be coupled to both chiralities of the muon. However, in this case there is no connection between the different observables. We refer the reader to Sec. 4 for more details.

In this case, the texture in Eq. (35) will lead to a prediction for the $t \rightarrow c\mu^+\mu^-$ or $t \rightarrow ce^+e^-$ decays⁴ according to the interaction mediated by $\phi_4^{5/3}$ in Eq. (18). Assuming naively $V_{\text{CKM}} \sim \mathbb{I}$,

⁴Similarly to the case of $B \rightarrow K\mu^\pm e^\mp$ previously discussed, there is freedom in the matrix entries to satisfy the experimental bound on $t \rightarrow c\mu^\pm e^\mp$.

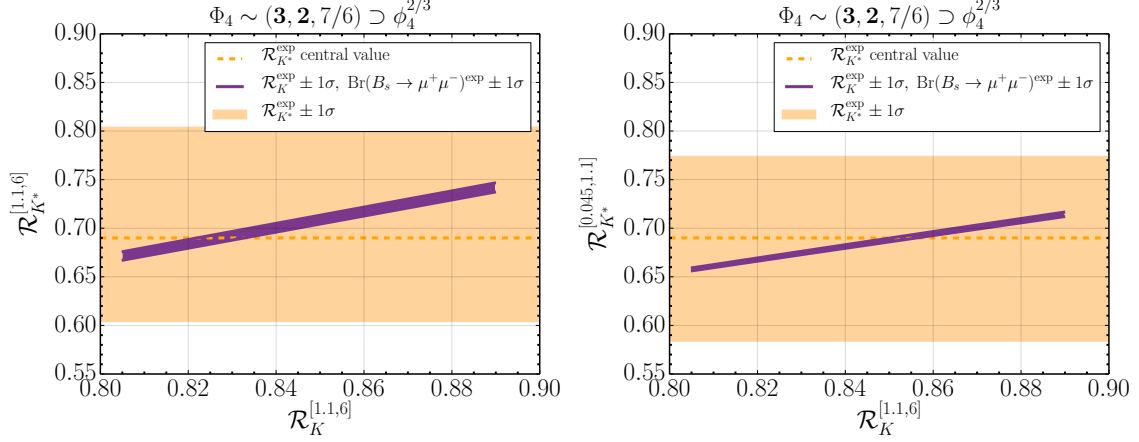


FIG. 5: The purple band gives the prediction for \mathcal{R}_{K^*} in the window $0.045 < q^2 < 1.1 \text{ GeV}^2$ (left panel) and $1.1 < q^2 < 6 \text{ GeV}^2$ (right panel) for the points satisfying $\mathcal{R}_K^{\text{exp}}$ and $\text{Br}(B_s \rightarrow \mu^+ \mu^-)^{\text{exp}}$ within 1σ . The region shaded in orange corresponds to the measurement of \mathcal{R}_{K^*} at 1σ .

the prediction for the branching fraction of the top decay into muons would be $\text{Br}(t \rightarrow c \mu^+ \mu^-) \sim 2 \times 10^{-7}$, which is consistent with the existing experimental constraints [53, 54]. As this example shows, the theory correlates different observables that could be tested in the near future.

4. THE $g - 2$ OF THE MUON

The Fermilab $g - 2$ experiment has recently reported results on the anomalous magnetic moment of the muon $a_\mu \equiv (g - 2)_\mu/2$ from their Run 1 [29]. The combined result with the one from the E821 experiment at BNL [30] deviates from the SM prediction by 4.2σ , as Eq. (2) manifests. In this section we show that in the most general case, the theory gives a prediction for $(g - 2)_\mu$ that can explain the reported deviation, involving the same leptoquarks in the theory that have been discussed so far.

In general, the $\text{SU}(2)_L$ field components from Φ_3 and Φ_4 with electric charge $Q = -2/3$ can mix through the following terms in the scalar potential:

$$V(H, \Phi) \supset \lambda_{H\Phi} \text{Tr}[H^\dagger \Phi H^\dagger \Phi]. \quad (36)$$

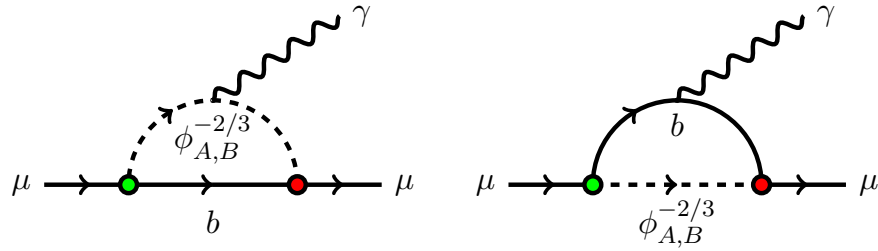


FIG. 6: Feynman diagrams for the topologies of the main contributions from the scalar leptoquarks to $(g - 2)_\mu$. The different colors in the vertices indicate opposite chiralities in the leptoquark - muon coupling.

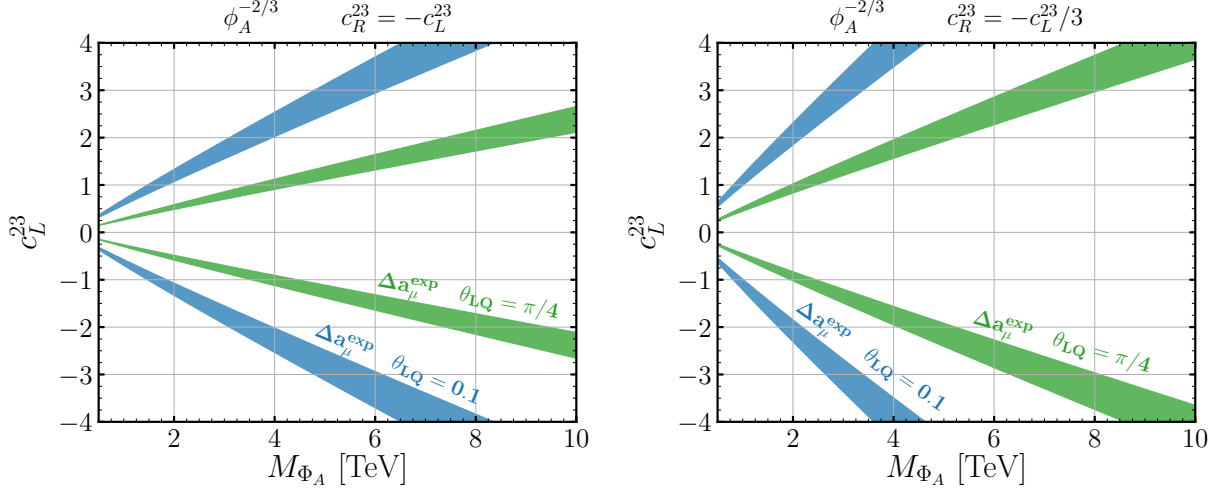


FIG. 7: Parameter space that explains the muon $g - 2$ anomaly in the c_L^{23} vs M_{Φ_A} plane; assuming that $c_R^{23} = -c_L^{23}$ (left panel) and $c_R^{23} = -c_L^{23}/3$ (right panel). The region shaded in blue (green) is in agreement with the combined result from the Muon $g - 2$ experiment at Fermilab and E821 at BNL for a mixing angle of $\theta_{LQ} = 0.1$ ($\theta_{LQ} = \pi/4$).

In the physical basis they can be written as a function of the mass eigenstates $\phi_A^{-2/3}$ and $\phi_B^{-2/3}$ as follows,

$$\begin{aligned}\phi_3^{-2/3} &= \cos \theta_{LQ} \phi_A^{-2/3} + \sin \theta_{LQ} \phi_B^{-2/3}, \\ (\phi_4^{2/3})^* &= -\sin \theta_{LQ} \phi_A^{-2/3} + \cos \theta_{LQ} \phi_B^{-2/3},\end{aligned}\tag{37}$$

where the angle θ_{LQ} parametrizes the scalar mixing. Therefore, the relevant Yukawa interactions for the $\phi_{A,B}^{-2/3}$ fields are given by

$$\begin{aligned}-\mathcal{L} \supset & \bar{e}^i \left(-\sin \theta_{LQ} c_L^{ij} P_L + \cos \theta_{LQ} c_R^{ij} P_R \right) d^j \phi_A^{-2/3} \\ & + \bar{e}^i \left(\cos \theta_{LQ} c_L^{ij} P_L + \sin \theta_{LQ} c_R^{ij} P_R \right) d^j \phi_B^{-2/3} + \text{h.c.},\end{aligned}\tag{38}$$

where the matrices $c_{L,R}$ correspond to

$$c_L^{ij} = (K_2^T V_{\text{CKM}} K_1^T V_6^T)^{ij}, \quad \text{and} \quad c_R^{ij} = (K_3 V_{\text{PMNS}} V_4^*)^{ij}.\tag{39}$$

Under the assumption that the New Physics couples mostly to muons, we adopt the simplest texture for these matrices needed to have a non-zero contribution to the observables involving $b \rightarrow s$ transitions,

$$c_{L,R} = \begin{pmatrix} 0 & 0 & 0 \\ 0 & c_{L,R}^{22} & c_{L,R}^{23} \\ 0 & 0 & 0 \end{pmatrix}.\tag{40}$$

The Feynman graphs for the two different topologies that lead to the main contributions to

$(g-2)_\mu$ are show in Fig. 6. These contributions can be written as

$$\begin{aligned} \Delta a_\mu^\alpha = & \frac{-3}{16\pi^2} \frac{m_\mu^2}{M_{\Phi_\alpha}^2} \sum_j \left[\left(|\lambda_{\alpha L}^{2j}|^2 + |\lambda_{\alpha R}^{2j}|^2 \right) \times (Q_d F_1(x_j^\alpha) + Q_\alpha F_2(x_j^\alpha)) \right. \\ & \left. + \frac{m_{q_j}}{m_\mu} \text{Re}[\lambda_{\alpha L}^{2j} (\lambda_{\alpha R}^{2j})^*] (Q_d F_3(x_j^\alpha) + Q_\alpha F_4(x_j^\alpha)) \right], \end{aligned} \quad (41)$$

where the loop-functions are given by

$$F_1(x) = \frac{1}{6(1-x)^4} (2 + 3x - 6x^2 + x^3 + 6x \ln x), \quad (42)$$

$$F_2(x) = \frac{1}{6(1-x)^4} (1 - 6x + 3x^2 + 2x^3 - 6x^2 \ln x), \quad (43)$$

$$F_3(x) = \frac{1}{(1-x)^3} (-3 + 4x - x^2 - 2 \ln x), \quad (44)$$

$$F_4(x) = \frac{1}{(1-x)^3} (1 - x^2 + 2x \ln x), \quad (45)$$

with $x_j^\alpha = (m_{q_j}/M_{\phi_\alpha})^2$ and $\alpha = A, B$. The $\lambda_{\alpha L, R}$ couplings in the above equation are given by

$$\lambda_{AL} = -c_L \sin \theta_{LQ}, \quad \lambda_{AR} = c_R \cos \theta_{LQ}, \quad (46)$$

$$\lambda_{BL} = c_L \cos \theta_{LQ}, \quad \lambda_{BR} = c_R \sin \theta_{LQ}. \quad (47)$$

We note that the only relevant contribution to the $(g-2)_\mu$ comes from the interaction of the leptoquark with both left-handed and right-handed couplings to leptons, since it is enhanced by the m_{q_j}/m_μ ratio as Eq. (41) shows, being m_{q_j} the mass of the quark running inside the loop⁵. In our case the magnetic moment of the muon will be dominated by the b -quark inside the loop

$$\Delta a_\mu \simeq -\frac{m_\mu m_b}{32\pi^2} \sin 2\theta_{LQ} c_L^{23} (c_R^{23})^* \left(\frac{1}{M_{\phi_A}^2} [F_3(x_b^A) + 2F_4(x_b^A)] - \frac{1}{M_{\phi_B}^2} [F_3(x_b^B) + 2F_4(x_b^B)] \right). \quad (48)$$

Assuming that $M_{\phi_B} \gg M_{\phi_A}$ we present in Fig. 7 the parameter space that explains the muon $g-2$ anomaly in the c_L^{23} vs M_{ϕ_A} plane; assuming that $c_R^{23} = -c_L^{23}$ (left panel) and $c_R^{23} = -c_L^{23}/3$ (right panel). The region shaded in blue (green) is in agreement with the combined result from the Muon $g-2$ experiment at Fermilab and E821 at BNL for a mixing angle of $\theta_{LQ} = 0.1$ ($\theta_{LQ} = \pi/4$). As one can appreciate, in this theory one can easily achieve the reported values for $(g-2)_\mu$.

A. Correlation between the Muon $g-2$ and $\mathcal{R}_{K^{(*)}}$

In this section we study the possibility to explain the \mathcal{R}_K and the $(g-2)_\mu$ anomalies simultaneously. For alternative solutions to both of these anomalies see e.g. Refs. [55–58]. As we have discussed in Sections 3 A and 3 B the Φ_3 leptoquark generates the C'_9 and C'_{10} Wilson coefficients while Φ_4 generates C_9 and C_{10} . In the scenario with mixing between them the following Wilson

⁵As one can also read from Eq. (41), when we consider Φ_3 and Φ_4 individually and neglect Y_2 this would require non-perturbative couplings or small masses (severely constrained by the LHC) to explain the reported deviation in $(g-2)_\mu$.

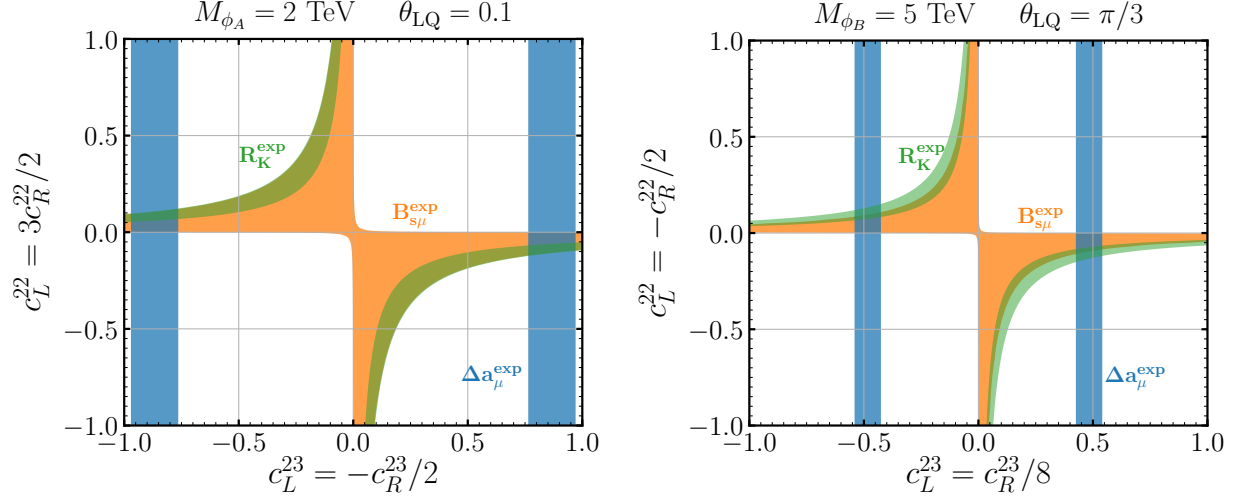


FIG. 8: Parameter space that explains the flavor and $(g-2)_\mu$ anomalies in the c_L^{22} vs c_L^{23} plane. The region shaded in blue is in agreement with the combined result from the Muon $g-2$ experiment at Fermilab and E821 at BNL within 1σ . The green (orange) band is in agreement with the measurement of \mathcal{R}_K ($\text{Br}(B_s \rightarrow \mu^+ \mu^-)$) within 1σ . In the left panel we consider the contribution from the ϕ_A leptoquark with $M_{\phi_A} = 2$ TeV and mixing angle $\theta_{LQ} = 0.1$. In the right panel we consider the contribution from the ϕ_B leptoquark with $M_{\phi_B} = 5$ TeV and mixing angle $\theta_{LQ} = \pi/3$.

operators also appear

$$\mathcal{L}_{\text{eff}}^{\phi_{A,B}} \supset \frac{4G_F}{\sqrt{2}} V_{tb} V_{ts}^* \frac{\alpha}{4\pi} [C_{S\ell\ell} (\bar{s} P_R b) (\bar{\ell} \ell) + C_{P\ell\ell} (\bar{s} P_R b) (\bar{\ell} \gamma^5 \ell)] + \text{h.c.}, \quad (49)$$

and the primed operators $C'_{S\ell\ell}$ and $C'_{P\ell\ell}$ are obtained by the replacement $P_R \leftrightarrow P_L$. In this section we focus on New Physics coupled to muons so we take $\ell = \mu$. Then, the contribution to the Wilson coefficients from the $\phi_A^{-2/3}$ and $\phi_B^{-2/3}$ relevant for the neutral anomalies correspond to

$$\frac{M_{\phi_A}^2}{\sin^2 \theta_{LQ}^2} C_{9A} = \frac{M_{\phi_A}^2}{\sin^2 \theta_{LQ}^2} C_{10A} = \frac{M_{\phi_B}^2}{\cos^2 \theta_{LQ}^2} C_{9B} = \frac{M_{\phi_B}^2}{\cos^2 \theta_{LQ}^2} C_{10B} = -\frac{c_L^{23} (c_L^{22})^*}{4} \frac{\sqrt{2}\pi}{G_F \alpha}, \quad (50)$$

$$\frac{M_{\phi_A}^2}{\cos^2 \theta_{LQ}^2} C'_{9A} = -\frac{M_{\phi_A}^2}{\cos^2 \theta_{LQ}^2} C'_{10A} = \frac{M_{\phi_B}^2}{\sin^2 \theta_{LQ}^2} C'_{9B} = -\frac{M_{\phi_B}^2}{\sin^2 \theta_{LQ}^2} C'_{10B} = -\frac{c_R^{23} (c_R^{22})^*}{4} \frac{\sqrt{2}\pi}{G_F \alpha}, \quad (51)$$

$$\frac{M_{\phi_A}^2}{\sin 2\theta_{LQ}} C_{SA} = \frac{M_{\phi_A}^2}{\sin 2\theta_{LQ}} C_{PA} = -\frac{M_{\phi_B}^2}{\sin 2\theta_{LQ}} C_{SB} = -\frac{M_{\phi_B}^2}{\sin 2\theta_{LQ}} C_{PB} = \frac{c_R^{23} (c_L^{22})^*}{8} \frac{\sqrt{2}\pi}{G_F \alpha}, \quad (52)$$

$$\frac{M_{\phi_A}^2}{\sin 2\theta_{LQ}} C'_{SA} = -\frac{M_{\phi_A}^2}{\sin 2\theta_{LQ}} C'_{PA} = -\frac{M_{\phi_B}^2}{\sin 2\theta_{LQ}} C'_{SB} = \frac{M_{\phi_B}^2}{\sin 2\theta_{LQ}} C'_{PB} = \frac{c_L^{23} (c_R^{22})^*}{8} \frac{\sqrt{2}\pi}{G_F \alpha}, \quad (53)$$

we consider the contributions from all these Wilson coefficients in our calculations of $\mathcal{R}_K^{(*)}$ and the branching ratio of $B_s \rightarrow \mu^+ \mu^-$.

Notice that the physical fields have interactions with both chiralities of the SM fermions; thus, there are new interactions which are proportional to $\sin 2\theta_{LQ}$. In other words, due to the scalar mixing we have new contributions from the scalar and pseudoscalar Wilson coefficients $C_{S'}$

and $C_{P^{(\prime)}}$. On the other hand, those new interactions arising from the effective Lagrangian that are proportional to the mixing are precisely the ones required to generate a relevant contribution to the $(g - 2)_\mu$, as we discussed above.

In Fig. 8 we show the parameter space that explains the flavor and $(g - 2)_\mu$ anomalies in the c_L^{22} vs c_L^{23} plane. The region shaded in blue is in agreement with the combined result from the Muon $g - 2$ experiment at Fermilab and E821 at BNL within 1σ . The green and orange bands are in agreement with the measurements of \mathcal{R}_K and $\text{Br}(B_s \rightarrow \mu^+\mu^-)$ within 1σ , respectively. For the figure in the left panel we consider $M_{\phi_B} \gg M_{\phi_A}$ such that the main contribution comes from ϕ_A . The mass of the scalar leptoquark and the mixing have been fixed to $M_{\phi_A} = 2$ TeV and $\theta_{LQ} = 0.1$. The Yukawa couplings are related as shown by the labels on the axes. As the figure shows, there is a region that simultaneously explains the measured values of \mathcal{R}_K , $\text{Br}(B_s \rightarrow \mu^+\mu^-)$ and $(g - 2)_\mu$ within 1σ . In this region of overlap the predicted values for \mathcal{R}_{K^*} correspond to $\mathcal{R}_{K^*}^{[1.1, 1.6]} \approx [1.1, 1.16]$ and $\mathcal{R}_{K^*}^{[0.045, 1.1]} \approx [0.98, 1.03]$ which are larger than the current experimental central value. The right panel in Fig. 8 shows our results for $M_{\phi_A} \gg M_{\phi_B}$ such that the main contribution comes from ϕ_B . The mass of the scalar leptoquark and the mixing have been fixed to $M_{\phi_B} = 5$ TeV and $\theta_{LQ} = \pi/3$. The Yukawa couplings are related as shown by the labels on the axes. For this case there is also a region that simultaneously explains the measured values of \mathcal{R}_K , $\text{Br}(B_s \rightarrow \mu^+\mu^-)$ and $(g - 2)_\mu$. In the region of overlap we obtain the same predictions for \mathcal{R}_{K^*} as for the case of ϕ_A .

5. SUMMARY

We have discussed the simplest quark-lepton unification theory that can be realized at the TeV scale [6]. This theory is based on the $\text{SU}(4)_C \otimes \text{SU}(2)_L \otimes \text{U}(1)_R$ gauge group and in order to have a consistent theory for fermion masses at the low scale, neutrino masses are generated through the inverse seesaw mechanism. This theory predicts the existence of a vector leptoquark, $X_\mu \sim (\mathbf{3}, \mathbf{1}, -2/3)_{\text{SM}}$, and two scalar leptoquarks, $\Phi_3 \sim (\bar{\mathbf{3}}, \mathbf{2}, -1/6)_{\text{SM}}$ and $\Phi_4 \sim (\mathbf{3}, \mathbf{2}, 7/6)_{\text{SM}}$, that can provide a relevant contribution to meson decays.

We have studied the possibility to explain the experimental values for the clean observables involving $b \rightarrow s$ transitions, i.e. \mathcal{R}_K , \mathcal{R}_{K^*} and $\text{Br}(B_s \rightarrow \mu^+\mu^-)$, in two main scenarios. In the first scenario the scalar leptoquark, Φ_3 , gives the main contributions to the relevant meson decays, while in the second scenario the scalar leptoquark, Φ_4 , plays the main role to explain the values for the neutral flavour anomalies. We demonstrated that in the most general case where there is mixing between the scalar leptoquarks there is a contribution to $(g - 2)_\mu$ that does not suffer from a chiral suppression, and hence, the experimental value can be explained without leading to strong experimental collider constraints. Consequently, we showed that the minimal theory for quark-lepton unification proposed in Ref. [6] can explain simultaneously the recent experimental results for \mathcal{R}_K and $(g - 2)_\mu$. We hope that, in the near future, more experimental data and an improvement on the theoretical predictions will determine whether these anomalies represent final evidence for New Physics, and whether the minimal theory for quark-lepton unification can be behind them by contrasting alternative predictions with experimental results.

Acknowledgments: The work of P.F.P. has been supported by the U.S. Department of Energy, Office of Science, Office of High Energy Physics, under Award Number DE-SC0020443. The work of C.M. is supported by the U.S. Department of Energy, Office of Science, Office of High Energy Physics, under Award Number DE-SC0011632 and by the Walter Burke Institute for Theoretical Physics.

A. Leptoquark Interactions

In our convention the mass matrices are diagonalized as

$$U^T M_U U_C = M_U^{\text{diag}}, \quad (\text{A1})$$

$$D^T M_D D_C = M_D^{\text{diag}}, \quad (\text{A2})$$

$$E^T M_E E_C = M_E^{\text{diag}}. \quad (\text{A3})$$

The following matrices enter in the leptoquark interactions below:

$$V_1 = N_C^\dagger U_C, \quad V_2 = E_C^\dagger D_C, \quad V_3 = U_L^T Y_2 N_C, \quad V_4 = N_C^T Y_4 D_C, \quad V_5 = N_L^T Y_2 U_C, \quad \text{and} \quad V_6 = U_L^T Y_4 E_C.$$

$$U_L^\dagger D_L = K_1 V_{\text{CKM}} K_2 \quad \text{and} \quad E_L^\dagger N_L = K_3 V_{\text{PMNS}}.$$

K_1 and K_3 are diagonal matrices containing three phases, while K_2 has two phases.

- Vector Leptoquark $X_\mu \sim (\mathbf{3}, \mathbf{1}, 2/3)_{\text{SM}}$:

$$\frac{g_4}{\sqrt{2}} \bar{d}_L V_{DE} \gamma^\mu e_L X_\mu, \quad (\text{A4})$$

$$\frac{g_4}{\sqrt{2}} \bar{u}_L (K_1 V_{\text{CKM}} K_2 V_{DE} K_3 V_{\text{PMNS}}) \gamma^\mu \nu_L X_\mu, \quad (\text{A5})$$

$$\frac{g_4}{\sqrt{2}} \overline{(\nu^c)}_L V_1 \gamma^\mu (u^c)_L X_\mu, \quad (\text{A6})$$

$$\frac{g_4}{\sqrt{2}} \overline{(e^c)}_L V_2 \gamma^\mu (d^c)_L X_\mu. \quad (\text{A7})$$

- Scalar Leptoquark $\Phi_3 \sim (\bar{\mathbf{3}}, \mathbf{2}, -1/6)_{\text{SM}}$:

$$u_L^T C V_3 (\nu^c)_L \phi_3^{-2/3}, \quad (\text{A8})$$

$$d_L^T C K_2 V_{\text{PMNS}}^T K_1 V_3 (\nu^c)_L \phi_3^{1/3}, \quad (\text{A9})$$

$$\nu_L^T C V_4 (d^c)_L (\phi_3^{1/3})^*, \quad (\text{A10})$$

$$e_L^T C K_3^* V_{\text{PMNS}}^* V_4 (d^c)_L (\phi_3^{-2/3})^*. \quad (\text{A11})$$

- Scalar Leptoquark $\Phi_4 \sim (\mathbf{3}, \mathbf{2}, 7/6)_{\text{SM}}$:

$$\nu_L^T C V_5 (u^c)_L \phi_4^{2/3}, \quad (\text{A12})$$

$$e_L^T C K_3^* V_{\text{PMNS}}^* V_5 (u^c)_L \phi_4^{5/3}, \quad (\text{A13})$$

$$u_L^T C V_6 (e^c)_L (\phi_4^{5/3})^*, \quad (\text{A14})$$

$$d_L^T C K_2 V_{\text{CKM}}^T K_1 V_6 (e^c)_L (\phi_4^{2/3})^*. \quad (\text{A15})$$

Notice that when $Y_2 \rightarrow 0$ the matrices $V_3 \rightarrow 0$ and $V_5 \rightarrow 0$.

[1] J. C. Pati and A. Salam, “Lepton Number as the Fourth Color,” *Phys. Rev. D* **10**, 275–289 (1974), [Erratum: *Phys.Rev.D* 11, 703–703 (1975)].

- [2] P. Minkowski, “ $\mu \rightarrow e\gamma$ at a Rate of One Out of 10^9 Muon Decays?” *Phys. Lett. B* **67**, 421–428 (1977).
- [3] T. Yanagida, “Horizontal gauge symmetry and masses of neutrinos,” *Conf. Proc. C* **7902131**, 95–99 (1979).
- [4] M. Gell-Mann, P. Ramond, and R. Slansky, “Complex Spinors and Unified Theories,” *Conf. Proc. C* **790927**, 315–321 (1979), [arXiv:1306.4669 \[hep-th\]](#).
- [5] R. N. Mohapatra and G. Senjanovic, “Neutrino Mass and Spontaneous Parity Nonconservation,” *Phys. Rev. Lett.* **44**, 912 (1980).
- [6] P. Fileviez Perez and M. B. Wise, “Low Scale Quark-Lepton Unification,” *Phys. Rev. D* **88**, 057703 (2013), [arXiv:1307.6213 \[hep-ph\]](#).
- [7] R. N. Mohapatra, “Mechanism for Understanding Small Neutrino Mass in Superstring Theories,” *Phys. Rev. Lett.* **56**, 561–563 (1986).
- [8] R. N. Mohapatra and J. W. F. Valle, “Neutrino Mass and Baryon Number Nonconservation in Superstring Models,” *Phys. Rev. D* **34**, 1642 (1986).
- [9] I. Doršner, S. Fajfer, A. Greljo, J. F. Kamenik, and N. Košnik, “Physics of leptoquarks in precision experiments and at particle colliders,” *Phys. Rept.* **641**, 1–68 (2016), [arXiv:1603.04993 \[hep-ph\]](#).
- [10] R. Aaij *et al.* (LHCb), “Test of lepton universality in beauty-quark decays,” (2021), [arXiv:2103.11769 \[hep-ex\]](#).
- [11] B. Gripaios, M. Nardecchia, and S. A. Renner, “Composite leptoquarks and anomalies in B -meson decays,” *JHEP* **05**, 006 (2015), [arXiv:1412.1791 \[hep-ph\]](#).
- [12] R. Alonso, B. Grinstein, and J. Martin Camalich, “Lepton universality violation and lepton flavor conservation in B -meson decays,” *JHEP* **10**, 184 (2015), [arXiv:1505.05164 \[hep-ph\]](#).
- [13] H. Päs and E. Schumacher, “Common origin of R_K and neutrino masses,” *Phys. Rev. D* **92**, 114025 (2015), [arXiv:1510.08757 \[hep-ph\]](#).
- [14] D. Bečirević, N. Košnik, O. Sumensari, and R. Zukanovich Funchal, “Palatable Leptoquark Scenarios for Lepton Flavor Violation in Exclusive $b \rightarrow s\ell_1\ell_2$ modes,” *JHEP* **11**, 035 (2016), [arXiv:1608.07583 \[hep-ph\]](#).
- [15] R. Barbieri, C. W. Murphy, and F. Senia, “B-decay Anomalies in a Composite Leptoquark Model,” *Eur. Phys. J. C* **77**, 8 (2017), [arXiv:1611.04930 \[hep-ph\]](#).
- [16] B. Capdevila, A. Crivellin, S. Descotes-Genon, J. Matias, and J. Virto, “Patterns of New Physics in $b \rightarrow s\ell^+\ell^-$ transitions in the light of recent data,” *JHEP* **01**, 093 (2018), [arXiv:1704.05340 \[hep-ph\]](#).
- [17] G. Hiller and I. Nisandzic, “ R_K and R_{K^*} beyond the standard model,” *Phys. Rev. D* **96**, 035003 (2017), [arXiv:1704.05444 \[hep-ph\]](#).
- [18] G. D’Amico, M. Nardecchia, P. Panci, F. Sannino, A. Strumia, R. Torre, and A. Urbano, “Flavour anomalies after the R_{K^*} measurement,” *JHEP* **09**, 010 (2017), [arXiv:1704.05438 \[hep-ph\]](#).
- [19] D. Buttazzo, A. Greljo, G. Isidori, and D. Marzocca, “B-physics anomalies: a guide to combined explanations,” *JHEP* **11**, 044 (2017), [arXiv:1706.07808 \[hep-ph\]](#).
- [20] L. Di Luzio, A. Greljo, and M. Nardecchia, “Gauge leptoquark as the origin of B-physics anomalies,” *Phys. Rev. D* **96**, 115011 (2017), [arXiv:1708.08450 \[hep-ph\]](#).
- [21] T. Faber, M. Hudec, M. Malinský, P. Meinzinger, W. Porod, and F. Staub, “A unified leptoquark model confronted with lepton non-universality in B -meson decays,” *Phys. Lett. B* **787**, 159–166 (2018), [arXiv:1808.05511 \[hep-ph\]](#).
- [22] O. Popov, M. A. Schmidt, and G. White, “ R_2 as a single leptoquark solution to $R_{D^{(*)}}$ and $R_{K^{(*)}}$,” *Phys. Rev. D* **100**, 035028 (2019), [arXiv:1905.06339 \[hep-ph\]](#).
- [23] S. Balaji and M. A. Schmidt, “Unified SU(4) theory for the $R_{D^{(*)}}$ and $R_{K^{(*)}}$ anomalies,” *Phys. Rev. D* **101**, 015026 (2020), [arXiv:1911.08873 \[hep-ph\]](#).
- [24] G. Hiller, D. Loose, and I. Nišandžić, “Flavorful leptoquarks at the LHC and beyond: Spin 1,” (2021), [arXiv:2103.12724 \[hep-ph\]](#).
- [25] W. Altmannshofer and P. Stangl, “New Physics in Rare B Decays after Moriond 2021,” (2021), [arXiv:2103.13370 \[hep-ph\]](#).
- [26] C. Cornella, D. A. Faroughy, J. Fuentes-Martín, G. Isidori, and M. Neubert, “Reading the footprints of the B-meson flavor anomalies,” (2021), [arXiv:2103.16558 \[hep-ph\]](#).
- [27] R. Fleischer, R. Jaarsma, and G. Tetlalmatzi-Xolocotzi, “Mapping out the Space for New Physics with Leptonic and Semileptonic $B_{(c)}$ Decays,” (2021), [arXiv:2104.04023 \[hep-ph\]](#).

- [28] D. Lancierini, G. Isidori, P. Owen, and N. Serra, “On the significance of new physics in $b \rightarrow s\ell^+\ell^-$ decays,” (2021), [arXiv:2104.05631 \[hep-ph\]](#).
- [29] B. Abi *et al.* (Muon g-2), “Measurement of the Positive Muon Anomalous Magnetic Moment to 0.46 ppm,” *Phys. Rev. Lett.* **126**, 141801 (2021), [arXiv:2104.03281 \[hep-ex\]](#).
- [30] G. W. Bennett *et al.* (Muon g-2), “Final Report of the Muon E821 Anomalous Magnetic Moment Measurement at BNL,” *Phys. Rev. D* **73**, 072003 (2006), [arXiv:hep-ex/0602035](#).
- [31] S. Borsanyi *et al.*, “Leading hadronic contribution to the muon 2 magnetic moment from lattice QCD,” (2020), [10.1038/s41586-021-03418-1](#), [arXiv:2002.12347 \[hep-lat\]](#).
- [32] A. Freitas, J. Lykken, S. Kell, and S. Westhoff, “Testing the Muon g-2 Anomaly at the LHC,” *JHEP* **05**, 145 (2014), [Erratum: *JHEP* 09, 155 (2014)], [arXiv:1402.7065 \[hep-ph\]](#).
- [33] W.-C. Chiu, C.-Q. Geng, and D. Huang, “Correlation Between Muon $g - 2$ and $\mu \rightarrow e\gamma$,” *Phys. Rev. D* **91**, 013006 (2015), [arXiv:1409.4198 \[hep-ph\]](#).
- [34] L. Calibbi, R. Ziegler, and J. Zupan, “Minimal models for dark matter and the muon g-2 anomaly,” *JHEP* **07**, 046 (2018), [arXiv:1804.00009 \[hep-ph\]](#).
- [35] R. Mandal and A. Pich, “Constraints on scalar leptoquarks from lepton and kaon physics,” *JHEP* **12**, 089 (2019), [arXiv:1908.11155 \[hep-ph\]](#).
- [36] I. Doršner, S. Fajfer, and O. Sumensari, “Muon $g - 2$ and scalar leptoquark mixing,” *JHEP* **06**, 089 (2020), [arXiv:1910.03877 \[hep-ph\]](#).
- [37] I. Bigaran and R. R. Volkas, “Getting chirality right: Single scalar leptoquark solutions to the $(g - 2)_{e,\mu}$ puzzle,” *Phys. Rev. D* **102**, 075037 (2020), [arXiv:2002.12544 \[hep-ph\]](#).
- [38] R. Capdevilla, D. Curtin, Y. Kahn, and G. Krnjaic, “A No-Lose Theorem for Discovering the New Physics of $(g - 2)_\mu$ at Muon Colliders,” (2021), [arXiv:2101.10334 \[hep-ph\]](#).
- [39] M. J. Baker, P. Cox, and R. R. Volkas, “Radiative Muon Mass Models and $(g - 2)_\mu$,” (2021), [arXiv:2103.13401 \[hep-ph\]](#).
- [40] M. A. Buen-Abad, J. Fan, M. Reece, and C. Sun, “Challenges for an axion explanation of the muon $g - 2$ measurement,” (2021), [arXiv:2104.03267 \[hep-ph\]](#).
- [41] D. W. P. Amaral, D. G. Cerdeño, A. Cheek, and P. Foldenauer, “Distinguishing $U(1)_{L_\mu - L_\tau}$ from $U(1)_{L_\mu}$ as a solution for $(g - 2)_\mu$ with neutrinos,” (2021), [arXiv:2104.03297 \[hep-ph\]](#).
- [42] Y. Bai and J. Berger, “Muon g-2 in Lepton Portal Dark Matter,” (2021), [arXiv:2104.03301 \[hep-ph\]](#).
- [43] P. Athron, C. Balázs, D. H. Jacob, W. Kotlarski, D. Stöckinger, and H. Stöckinger-Kim, “New physics explanations of a_μ in light of the FNAL muon $g - 2$ measurement,” (2021), [arXiv:2104.03691 \[hep-ph\]](#).
- [44] A. D. Smirnov, “The Minimal quark - lepton symmetry model and the limit on Z-prime mass,” *Phys. Lett. B* **346**, 297–302 (1995), [arXiv:hep-ph/9503239](#).
- [45] M. Beneke, C. Bobeth, and R. Szafron, “Power-enhanced leading-logarithmic QED corrections to $B_q \rightarrow \mu^+\mu^-$,” *JHEP* **10**, 232 (2019), [arXiv:1908.07011 \[hep-ph\]](#).
- [46] C. Bobeth, M. Gorbahn, T. Hermann, M. Misiak, E. Stamou, and M. Steinhauser, “ $B_{s,d} \rightarrow l^+l^-$ in the Standard Model with Reduced Theoretical Uncertainty,” *Phys. Rev. Lett.* **112**, 101801 (2014), [arXiv:1311.0903 \[hep-ph\]](#).
- [47] R. Fleischer, R. Jaarsma, and G. Tetlalmatzi-Xolocotzi, “In Pursuit of New Physics with $B_{s,d}^0 \rightarrow \ell^+\ell^-$,” *JHEP* **05**, 156 (2017), [arXiv:1703.10160 \[hep-ph\]](#).
- [48] J. A. Bailey *et al.*, “ $B \rightarrow Kl^+l^-$ Decay Form Factors from Three-Flavor Lattice QCD,” *Phys. Rev. D* **93**, 025026 (2016), [arXiv:1509.06235 \[hep-lat\]](#).
- [49] A. Bharucha, D. M. Straub, and R. Zwicky, “ $B \rightarrow V\ell^+\ell^-$ in the Standard Model from light-cone sum rules,” *JHEP* **08**, 098 (2016), [arXiv:1503.05534 \[hep-ph\]](#).
- [50] R. Aaij *et al.* (LHCb), “Measurement of the $B_s^0 \rightarrow \mu^+\mu^-$ branching fraction and effective lifetime and search for $B^0 \rightarrow \mu^+\mu^-$ decays,” *Phys. Rev. Lett.* **118**, 191801 (2017), [arXiv:1703.05747 \[hep-ex\]](#).
- [51] T. Aaltonen *et al.* (CDF), “Search for the Decays $B_s^0 \rightarrow e^+\mu^-$ and $B_s^0 \rightarrow e^+e^-$ in CDF Run II,” *Phys. Rev. Lett.* **102**, 201801 (2009), [arXiv:0901.3803 \[hep-ex\]](#).
- [52] R. Aaij *et al.* (LHCb), “Test of lepton universality with $B^0 \rightarrow K^{*0}\ell^+\ell^-$ decays,” *JHEP* **08**, 055 (2017), [arXiv:1705.05802 \[hep-ex\]](#).
- [53] M. Aaboud *et al.* (ATLAS), “Search for flavour-changing neutral current top-quark decays $t \rightarrow qZ$ in proton-proton collisions at $\sqrt{s} = 13$ TeV with the ATLAS detector,” *JHEP* **07**, 176 (2018), [arXiv:1803.09923 \[hep-ex\]](#).

- [54] M. Chala, J. Santiago, and M. Spannowsky, “Constraining four-fermion operators using rare top decays,” *JHEP* **04**, 014 (2019), [arXiv:1809.09624 \[hep-ph\]](#).
- [55] S. Saad, “Combined explanations of $(g - 2)_\mu$, $R_{D^{(*)}}$, $R_{K^{(*)}}$ anomalies in a two-loop radiative neutrino mass model,” *Phys. Rev. D* **102**, 015019 (2020), [arXiv:2005.04352 \[hep-ph\]](#).
- [56] D. Huang, A. P. Morais, and R. Santos, “Anomalies in B -meson decays and the muon $g - 2$ from dark loops,” *Phys. Rev. D* **102**, 075009 (2020), [arXiv:2007.05082 \[hep-ph\]](#).
- [57] A. Greljo, P. Stangl, and A. E. Thomsen, “A Model of Muon Anomalies,” (2021), [arXiv:2103.13991 \[hep-ph\]](#).
- [58] D. Marzocca and S. Trifinopoulos, “A Minimal Explanation of Flavour Anomalies: B-Meson Decays, Muon Magnetic Moment, and the Cabbibo Angle,” (2021), [arXiv:2104.05730 \[hep-ph\]](#).